PSR Report 2273

PERFORMANCE PREDICTIONS FOR A LONG-STANDOFF-RANGE INFRARED IMAGING SENSOR

P. M. Moser

April 1992

Phase Report
Contract N62269-90-C-0551

REPORT DOCUMENTATION PAGE

1. REPORT DATE (DD-MM-YYYY)	2. REPORT TYPE	3. DATES COVERED (From - To)
xx-04-1992	Phase Technical	To April 1992

4. TITLE AND SUBTITLE
Performance Predictions for a Long-Standoff-Range Infrared Imaging Sensor

5a. CONTRACT NUMBER
N62269-90-C-0551

5b. GRANT NUMBER

5c. PROGRAM ELEMENT NUMBER

6. AUTHOR(S)
Moser, Paul M.

5d. PROJECT NUMBER

5e. TASK NUMBER

5f. WORK UNIT NUMBER

7. PERFORMING ORGANIZATION NAME(S) AND ADDRESS(ES)
Pacific-Sierra Research Corporation
Warminster, PA 18974

8. PERFORMING ORGANIZATION REPORT NUMBER
PSR Report 2273

9. SPONSORING/MONITORING AGENCY NAME(S) AND ADDRESS(ES)
Naval Air Warfare Center Aircraft Division Warminster
Warminster, PA 18974

10. SPONSOR/MONITOR'S ACRONYM(S)
NAWCADWAR

11. SPONSOR/MONITOR'S REPORT NUMBER(S)

12. DISTRIBUTION/AVAILABILITY STATEMENT
Approved for public release, distribution unlimited

13. SUPPLEMENTARY NOTES
See also PSR Report 2248, "Performance Requirements for Long-Standoff-Range Infrared Imaging Sensor" by the same author.

14. ABSTRACT

The U.S. Navy is sponsoring a development directed toward upgrading the Air Force Electro-Optical Long Range Oblique Photography System (EO-LOROPS) to provide an additional nighttime infrared (IR) capability. In a previous study, PSR Report 2248, potential mission applications for IREO-LOROPS were proposed and discussed and a set of operational performance "requirements" was established. The present study was undertaken to investigate the extent to which this development could achieve those objectives.

15. SUBJECT TERMS
Long Range, Oblique, Photography, Infrared, Electro-Optical, Airborne, Nighttime

16. SECURITY CLASSIFICATION OF:			17. LIMITATION OF ABSTRACT	18. NUMBER OF PAGES	19a. NAME OF RESPONSIBLE PERSON
a. REPORT	b. ABSTRACT	c. THIS PAGE			19b. TELEPHONE NUMBER (Include area code)
unclassified	unclassified	unclassified	unlimited	27	

Standard Form 298 (Rev. 8/98)

CONTENTS

INTRODUCTION

Loral Fairchild Systems (LFS) has performed a study[1] directed toward upgrading the Air Force Electro-Optical Long Range Oblique Photography System (EO-LOROPS), to provide an additional nighttime infrared (IR) capability for the Navy. In another investigation,[2] performance "requirements" were postulated for such a sensor, based on a variety of potential Navy targets, operating environments and scenarios. The purpose of the present report is to predict the performance of the proposed IREO-LOROPS in the context of the previously stated requirements.

DESIGN/PERFORMANCE ASSUMPTIONS

The proposed imaging sensor would utilize a detector array consisting of 48,000 elements (3000 columns by 16 time-delay-and-integration (TDI) stages) in an optical system of 66-inch focal length and 12-inch diameter collecting aperture. The center-to-center spacing of the detector elements would be 40 micrometers, providing a nominal resolution of 23.86 microradians or a Nyquist angular frequency of 20.96 cycles per milliradian. Figure 1 is a plot of the predicted minimum resolvable temperature difference (MRT) under laboratory conditions for two scene background temperatures, based on LFS data.[1] MRT represents the smallest temperature difference for which the heated (cooled) bars of a standard four-bar target array are barely resolvable (50% probability) against their ambient temperature background as a function of the angular frequency of the bars subtended at the sensor. Figure 1 describes resolution-sensitivity performance for the case of no atmospheric transmission losses and no degrading effects of motion such as vibration.

APPROACH

The approach taken herein is to determine the angular frequency response required by the sensor as a function of target size and range and the task to be performed and to determine, by use of the MRT curves, the corresponding target-to-background temperature differences that would enable the sensor to resolve such angular frequencies. The resulting MRT values are then doubled to increase the probability of being able to perform the task successfully to 96% (high confidence) from 50% (barely achievable). The MRT is then multiplied by an additional factor (of about 3 to 5) to account for atmospheric transmission losses. The resulting value, roughly 6 to 10 times the MRT at the required spatial frequency, is then compared with statistical

1

values of target-to-background temperature difference to determine the percentage of time that the assumed task can be performed.

TARGET SET

Four categories of targets were selected: ships, land vehicles, other (mostly fixed) land targets, and aircraft on the ground. Dimensions of the targets were taken from Shumaker et al.[3] Regardless of its shape, each target was represented as a rectangular parallelepiped viewed broadside (beam aspect) at a depression angle of $20.05°$, an angle corresponding to an aircraft altitude of 12 km (39,370 ft) and a slant range of 35 km (18.9 nmi). For cases corresponding to shorter ranges, the assumed altitude and slant range were scaled proportionally to maintain a constant depression angle of $20.05°$. This was done to permit using range-independent values of effective projected area for each target. The "critical dimension" for each target was taken as the square root of its effective projected area in accordance with the procedures of Shumaker et al.[3] Table 1 lists the 14 selected targets, the length, width, and height of the rectangular parallelepiped into which each could be "boxed," their effective projected areas, and their critical dimensions.

RECOGNITION, CLASSIFICATION AND IDENTIFICATION CRITERIA

The criteria applied to "recognition" and "identification" of targets on land are those of Johnson as summarized by Shumaker et al.[3] In this sense, "recognition" implies the ability to distinguish the target from similarly classed military targets, such as distinguishing an army tank from an armored personnel carrier, both of which fall within the more general class of land vehicles. "Identification" implies the ability to determine the specific military designation of a target, such as distinguishing a T-62 tank from an M60 tank. In an operational situation, if it is known a priori that only enemy forces are occupying a given area, satisfying the criterion for recognition may be sufficient and, in this case, would provide information on what weapon to select, e.g., a Maverick missile against a tank. If there is some question about whether certain supposed targets are hostile or friendly, (for example, tanks in the Iraqi desert during Desert Storm) the more demanding criterion for "identification" may have to be invoked to reduce the likelihood of fratricide.

For targets on land, the Johnson criterion of 4.0 cycles/critical dimension (8.0 resolvable pixels/critical dimension) was selected for the task of recognition; for the task of identification, 6.4 cycles/critical dimension (12.8 resolvable pixels/critical dimension) was chosen. Rosell[4] provides words of caution on the use of such criteria

citing a high level of variability in the ability of an observer to perform target classification tasks. Rosell gives a range of values of 2 to 10 cycles/critical dimension for recognition and of 4.5 to 15 cycles/critical dimension for identification. In this report it is assumed that the selected criteria correspond to a 50% probability of being able to perform the task.

The Johnson criteria have been shown not to work well for ship targets, particularly when the smallest average projected dimension is taken as the critical dimension.[5] That is, because the average height of a ship, when viewed from the beam aspect, is typically less than its minimum dimension when viewed from the bow aspect, one would conclude, incorrectly, that a ship can be classified more easily from the bow aspect than from the beam aspect. To circumvent this problem, Moser[5] established criteria based upon the number of resolvable pixels falling on the projected area of the ship. He concluded that 66 pixels on target was sufficient for "classification," which he regarded as the ability to distinguish warships from merchant ships by differences in the characteristic outlines of their superstructures; he further concluded that 400 resolvable pixels on target was sufficient for "identification," that is, for example, to distinguish a Kotlin class destroyer from a Forrest Sherman class destroyer.

Figures 2 and 3 illustrate how the distinguishing information contained in ship silhouettes increases as the number of pixels on target. These figures also show how "picture quality" varies as a function of angular frequency at an arbitrary range of 20 nmi. For example, if the sensor MRT, the target-to-background temperature difference, and the atmospheric transmittance over a 20-nmi path enable an angular resolution of 10.3 cycles/mrad, the sensor should be capable of producing a picture of the quality of the seventh drawing from the top in each of figures 2 and 3. These particular pictures represent imagery in which about 360 resolvable pixels fall on the target; this nearly satisfies the criterion value (400) for "identification." (It is suggested that the reader view these block-type silhouettes at a distance of about 1500 times the pixel size of each particular image to allow the eye to filter out the high-frequency sampling noise generated in the drawing process. Under such viewing conditions all of the images below the reference image will appear to be of the same quality as the reference image because the angular frequency response of the eye limits the perceived resolution of the image.)

If, in applying the Johnson criteria, the critical dimension is taken as the square root of projected target area, the Johnson criteria reduce to a special case of the Moser criteria. Stated in terms of pixels per target area, the Johnson criteria become 64 (8^2) for recognition and 164 (12.8^2) for identification.

TARGET ANGULAR FREQUENCIES

The resolution demands imposed on an imaging sensor can be expressed in terms of angular frequency, with higher frequencies associated with smaller targets at longer ranges and the more challenging classification tasks.

Figure 4 is a plot of angular frequencies required for recognition of "generic" targets at the 50% probability level as a function of range for critical dimensions of 5, 10, 15, 20, 25, and 30 m. The equation used to generate these curves is

$$f = n\, r\, A^{-\frac{1}{2}} = n\, r/(C.D.)$$

in which f is the angular frequency, n is the criterion number of resolvable cycles across the critical dimension C.D. in m, r is the range in km, and A is the effective projected area of the target in m^2. For figure 4, a value of n = 4 was assumed. The Nyquist resolution limit (20.96 cycles/mrad) for IREO LOROPS is also shown.

It can be seen, for example, that for a target of C.D. = 5 m (corresponding roughly to a T-62 tank viewed broadside at a depression angle of 20.05 degrees), there is a possibility of recognizing the target out to a range of 26 km (14 nmi), provided an adequate target-to-background temperature difference exists (of the order of 15 C° (27 F°). At a range of 12.5 km (6.7 nmi), this 5-m target would require an angular frequency of 10 cycles/mrad. If this value is then inserted into the IREO LOROPS MRT curve (figure 1) for a 280-K background, one obtains MRT = 0.3 K = 0.3 C° = 0.54 F°. (Basically this means that one could barely resolve the four bars of a standard MRT pattern situated at the target location provided the width of each bar is 0.625 m, the bars differ in temperature from their background by 0.3 C°, and there is no atmospheric transmission loss.) One next doubles this value to convert from minimum resolvable temperature difference to "confidently" resolvable temperature difference. If one assumes that atmospheric transmission over this path is 25%, the MRT value read from figure 1 must be multiplied by an additional factor of 4. Thus, for this particular example, the target must differ from its background by 2 x 4 x 0.3 C° = 2.4 C° = 4.3 F°. The assumed background temperature of 280 K = 7°C = 44°F corresponds to the average nighttime temperature at Hannover, Germany, during May 1970 according to figure 40 of reference 2. Figure 10 of reference 2 indicates that, under clear springtime conditions in central Europe, the temperature difference between a tank and its background will exceed 2.4 C° about eight hours per night. Thus, with IREO LOROPS, one should be able to distinguish, at the 50% probability level, a tank (such as a T-62) from other military vehicles of comparable size, from a slant range of 6.7 nmi for 8 hours per night during clear weather in the spring in central Europe. For

the otherwise same set of conditions, this task could be accomplished throughout all hours of summer nights but for only about four hours per night during winter.

The foregoing discussion was undertaken to illustrate the various factors that play a rôle in determining what kind of performance can be expected. The reader is invited to explore other combinations of parameters and to perform "what if?" analyses.

Angular frequencies required for performing tasks of recognition/classification and identification as a function of range for the specific targets listed in table 1 are given in figures 5, 6, 7, and 8. The equation used to generate these curves is

$$f = 6.08 \, n \, r \, A^{-\frac{1}{2}} = 6.08 \, n \, r/(C.D.)$$

in which f is the angular frequency, n is the criterion number of resolvable cycles across the critical dimension C.D. in ft, r is the range in nmi, and A is the effective projected area of the target in ft^2. The Nyquist limit of 20.96 cycles/mrad, which represents an upper limit of performance for IREO LOROPS regardless of target intensity, equipment thermal sensitivity, and atmospheric transmission, is shown on figure 5. The interested reader can apply the procedures discussed above for the case of generic targets to the specific targets identified in figures 5, 6, 7, and 8.

Large targets such as the Pahlevi Dam and the Golden Gate Bridge should be recognizable in clear weather at ranges far in excess of 40 nmi, but gaining such imagery would, in itself, be of little tactical value. However, if one needed real-time battle damage assessment of such targets that had been attacked at night, one could use IREO LOROPS. If, for example, one wanted to determine if 5-m (16.4-ft) size holes had been blasted into the face of Pahlevi Dam, one could refer to figure 4 and conclude that the reconnaissance aircraft would have to penetrate to within about 10 to 15 km (5.4 to 8.1 nmi) to recognize the damage.

ATMOSPHERIC TRANSMISSION

In the earlier section entitled "APPROACH," it was stated that, in making performance estimates, one should introduce a factor of about 3 to 5 for atmospheric transmission losses. Figures 9 and 10 are calculated spectral transmittances for three values of slant range and two values of near-ground-level visibility. (The particular values were selected to permit correlation with figure 3.2.2-2 of reference 1.) Transmittance curves were computed for slant ranges of 35 km (18.9 nmi), 17.5 km (9.4 nmi), and 8.75 km (4.7 nmi) from altitudes of 12 km (39,370 ft), 6 km (19,685 ft), and 3 km (9,843 ft), respectively, all of which correspond to the same depression angle

of $20.05°$. In figures 9 and 10 it is seen that the average transmittance over these slant paths to the surface is relatively independent of slant range and visibility. That is, for a visibility of 25 km (13.5 nmi), the average transmittances (figure 9) for these three slant ranges over the 3.4- to 5.0-μm band are 33.8%, 35.7%, and 39.7%, respectively. For a visibility of 5 km, the average transmittances (figure 10) over the same slant ranges for the same band are 17.3%, 18.4% and 20.5%, respectively. Thus, even though the slant range varies by a factor of four, the average transmittance varies by less 10% relative to the mean for each visibility value. Even though the visibility varies by a factor of five, the mean transmittance varies by less than a factor of two. There are several reasons for this. First, most of the attenuation occurs at low altitude; thus, for a slant path to the surface, it makes little difference if the sensor altitude is 40,000 ft or 10,000 ft. Therefore, there is little to be gained, as far as atmospheric transmission is concerned, by reducing the operating altitude within this range. The effect of a visibility change is relatively small because visibility is reckoned over a near-surface horizontal path; in the case in question, the surface is viewed at the end of an oblique path which does not include a large path through low-altitude haze. Furthermore, the dominant molecular absorber in the 3.4- to 5.0-μm band is carbon dioxide. CO_2 is such a strong absorber in the region of 4.3 μm that, even over very short paths (i.e., tens of meters), it absorbs almost 100% of the incident radiation, resulting in relatively small incremental changes as the path length is further increased.

Ideally, one should not treat atmospheric transmittance independently as a single number but rather in conjunction with other parameters that also exhibit a spectral dependence, such as detector responsivity, transmission of the optical system, and the thermal derivative of the spectral radiant emittance of the target. For example, the responsivity of platinum silicide decreases by almost an order of magnitude with increasing wavelength over the 3.4- to 5.0-μm band. However, this is off-set by an order of magnitude increase in the thermal derivative of the spectral radiant emittance of a blackbody with increasing wavelength over this band. Thus, if the spectral response of the optics is flat over the band, the spectral response of the system will be similar to the spectral atmospheric transmittance.

Figures 9 and 10 illustrate that over the wavelength interval of 4.2 to 4.6 μm, virtually no radiation from the scene reaches the detector array because of molecular absorption in the intervening atmosphere. At wavelengths for which the atmosphere is a strong absorber, it is also a strong radiator. Thus, CO_2 at a temperature of say, 280 K, is a strong emitter at wavelengths in the vicinity of 4.3 μm. However, if the sensor is at high altitude, where the temperature may be about 220 K, this 4.3-μm radiation will be absorbed by the cold CO_2 at that altitude but very little will be emitted. Thus one needn't be too concerned about noise contributed by 4.3-μm photons generated by the background scene or the atmosphere (for high altitude operation). However, within the

6

sensor itself, photons are produced within this band which contribute noise but no signal. If a cooled filter with a low insertion loss could be installed at the detector location, system sensitivity could be improved. The filter could be tailored to match the absorption band centered at about 4.3 μm or it may be more efficient simply to filter out all wavelengths greater than about 4.2 μm.

In reference 2, visibility data were provided for a single site, namely, Hannover, Germany. Some additional data from references 6, 7, and 8 have now been plotted to yield curves of cumulative frequencies of occurrence of various values of visibility for six marine locations. The data, which are presented in figures 11 through 16, are considerably less pessimistic than the Hannover data and show, for example, that the visibility is less than 5 nmi between 15 and 20 percent of the time at sites in the Norwegian Sea and off Boston, MA. For the sites selected, visibility improves with decreasing latitude to the extent that in the vicinity of Key West, FL, visibility less than 5 nmi occurs only 0.8 % of the time.

The values of visibility for which spectral transmittance of the atmosphere are plotted in figures 9 and 10 are 25 km (13.5 nmi) and 5 km (2.7 nmi), respectively. From figure 12 one can see that for the marine area off Boston, more than half the time the visibility is poorer than 25 km and about 12% of the time it is poorer than 5 km.

SAMPLE PERFORMANCE PREDICTIONS

There is a staggering number of combinations of the various parameters that govern the performance of an infrared imaging system. Examples of these parameters are the type of target, its orientation relative to the sensor, its temperature relative to its background, the temperature of the background, intra-target temperature differences, properties of the atmosphere that affect transmission (e.g., water vapor and aerosols), length of viewing path, sensor altitude and depression angle, sensor performance parameters such as MRT, the nature of the task to be performed, and image-quality criteria that determine the ability of an observer to perform the task. To make the problem tractable, single reasonable values were assumed for most of these parameters.

As discussed previously, it is assumed that the targets are always viewed broadside (generally the most favorable aspect angle) and always from a depression angle of 20.05° to maintain a constant effective projected area presented by each target to the sensor. Choice of such a line of sight made reasonable the use of the single value of atmospheric transmittance of 25% for slant paths of any length greater than 8.75 km (4.72 nmi) for visibilities ranging from 5 km (2.7 nmi) to 25 km (13.5 nmi). Accordingly, the laboratory values of sensor MRT for a scene background temperature of 280 K

were multiplied by a factor of four to allow for atmospheric transmission losses. The sensor was assumed to be perfectly stable and free of all effects of unsteadiness. For targets on land, the Johnson criteria for recognition and identification were used; the critical dimension was taken as the square root of the target's effective projected area. For ship targets, the Moser criteria for classification and identification were used. Calculations were performed for two values of target-to-background temperature difference: $1\,C°$ and $2\,C°$. According to figure 3 of reference 2, these values are equalled or exceeded by ships at night 82% and 65% of the time, respectively.

Results of the range calculations are given in table 2. The targets are grouped into their four categories and, for the most part, are in order of increasing size. It is tacitly assumed that there are no impediments to proper operation of the equipment at altitudes as low as about 3000 ft and at slant ranges as short as about 1.4 nmi. (For example, it is assumed that the sensor has sufficiently high v/r capability to cope with such short ranges at reasonable aircraft speeds and that focus will be correctable, if necessary, for the short ranges.)

For the land vehicles, most of the recognition and identification ranges are shown to be less than 4 nmi, which falls outside the range envelope for which 25% atmospheric transmission was considered to be a reasonable value. For the case of high visibility (e.g., 25 km), these predicted range values are probably low by about 50%.

For the assumed constant depression angle of $20.05°$, the aircraft altitude equals 34% of the slant range to the surface. For the large land targets such as the Golden Gate Bridge and Pahlevi Dam (Iran), the ranges are so large the sensor aircraft would have to climb to satellite orbital altitudes to satisfy the assumed conditions. If the aircraft were to limit its altitude to about 40,000 ft, the sensor depression angle would have to be reduced to about $4°$ or less to accommodate such long ranges. However, this would increase the line-of-sight path length through the lower, more dense parts of the atmosphere and result in range reductions.

The use of simplifying assumptions in exercising the performance models has probably resulted in overestimating realizable performance against the very large targets and underestimating performance against the small targets.

CONCLUSIONS

In reference 2, potential mission applications for IREO LOROPS were proposed and discussed. Most of these involved the use of near-real-time infrared imaging to perform tasks that couldn't be performed better by other current means, such as

observing activities of third world countries taking place under cover of darkness. Pre-hostility activities would generally revolve about relatively small, transient, mobile/relocatable targets such as boats, tanks, trucks, and missile launchers. (Large fixed targets have such long time constants that they can be observed by a variety of other sensors.) If and when hostilities begin, there will be a need for infrared imagery for nighttime near-real-time battle damage assessment to avoid calling strikes against targets that have already been destroyed, and to identify forces, such as columns of tanks, as being friendly or enemy forces to avoid fratricide. Even if BDA is sought for easily imaged large targets, such as power stations, bridges and dams, the outward evidence of critical damage resulting from "surgical" strikes may be so subtle that imagery of high ground resolution is required to sense it.

It appears that IREO LOROPS, as presently proposed, will generally be unable to acquire needed information about small, mobile/relocatable targets at long standoff ranges (of the order of 20 nmi). Although the design resolution of IREO LOROPS is consistent with the state of the art, that resolution will not be realized most of the time in real-world situations because of its low sensitivity at the higher angular frequencies. (You can have all the resolution in the world, but it won't help you if you don't have enough sensitivity to use it.)

IREO LOROPS is being designed to provide a Nyquist-limited angular resolution of about 21 cycles/mrad; however, the thermal contrasts of representative targets viewed through an attenuating atmosphere limit its effective angular resolution to about one-fourth to one-half of that value. To enable the sensor to utilize its maximum design resolution in real-world situations, target-to-background temperature differences of the order of eight times the MRT at the Nyquist angular frequency are required. From the 280-K-background MRT curve of figure 1, it can be seen that unrealistically large target-to-background temperature differences of the order of $8 \times 1.8 \, K = 14.4 \, C^\circ = 25.9 \, F^\circ$ are required to exploit the full nominal resolution capability of the sensor. If the MRT of IREO LOROPS at the Nyquist angular frequency could be reduced from its current design value of 1.8 K to about 0.2 K (a factor of 9 increase in sensitivity) the usable resolution would be increased by a factor of two to four and an optimum match of resolution and sensitivity would be achieved.

ACKNOWLEDGEMENT

9

REFERENCES

1. Loral Fairchild Systems Review Draft of Final Report "DoN EO-LOROPS Image Sensor IR Retrofit, AN/AVD-5 IR Upgrade Evaluation," 13 January 1992

2. P. M. Moser, "Performance Requirements for Long-Standoff-Range Infrared Imaging Sensor," PSR Report 2248, February 1992

3. D. L. Shumaker, J. T. Wood and C. R. Thacker, "FLIR Performance Handbook," DCS Corporation, Alexandria, VA 22314

4. F. A. Rosell and G. L. Harvey, Editors, "The Fundamentals of Thermal Imaging Systems," NRL Report 8311, AD-A073763, 10 May 1979

5. P. M. Moser, "Mathematical Model of FLIR Performance," Naval Air Development Center Technical Memorandum NADC-20203A:PMM, AD-A045247, 19 October 1972

6. U.S. Naval Weather Service Command, "U.S. Navy Marine Climatic Atlas of the World, Volume I, North Atlantic Ocean, NAVAIR 50-1C-528, December 1974

7. U.S. Naval Weather Service Command, "Summary of Synoptic Meteorological Observations, North American Coastal Marine Areas, Volume 2" (Boston, Quonset Point, New York, Atlantic City), AD-707699, May 1970

8. U.S. Naval Weather Service Command, "Summary of Synoptic Meteorological Observations, North American Coastal Marine Areas, Volume 4" (Jacksonville, Miami, Key West), AD-707701, May 1970

Table 1.   SELECTED TARGETS AND THEIR DIMENSIONS

Target	Length (ft)	Width (ft)	Height (ft)	Projected Area* (ft²)	Critical Dimension (ft)
Datsun Pickup	15	5	5	96	9.8
BMP-1 APC	22	10	7	220	14.8
T-62 Tank	22	11	8	248	15.8
M60 Tank	23	12	11	332	18.2
Huey Cobra Helicopter	53	3	13	702	26.5
F-4 Aircraft	63	39	16	1789	42.3
TU-16 Aircraft	120	110	35	8471	92.0
C-5A Aircraft	248	223	65	34,104	184.7
Patrol Boat	80	20	12	1450	38.1
Destroyer Class Ship	400	42	24	14,778	121.6
Field Trailer	59	10	10	757	27.5
POL Storage Tank	39	39	59	2683	51.8
Pahlevi Dam	696	-	669	437,403	661.4
Golden Gate Bridge	6473	-	745	4,530,100	2128.4

* Viewed broadside at 20.05° depression angle

Table 2. PREDICTED RECOGNITION / CLASSIFICATION AND IDENTIFICATION RANGES FOR IREO LOROPS AGAINST VARIOUS TARGETS FOR TARGET-TO-BACKGROUND TEMPERATURE DIFFERENCES OF 1 C° AND 2 C°

TARGET	RECOGNITION / CLASSIFICATION RANGE (nmi)		IDENTIFICATION RANGE (nmi)	
	ΔT = 1 C°	ΔT = 2 C°	ΔT = 1 C°	ΔT = 2 C°
Datsun Pickup	2.2	3.6	1.4	2.3
BMP-1 APC	3.4	5.5	2.1	3.4
T-62 Tank	3.6	5.8	2.2	3.6
M60 Tank	4.1	6.7	2.6	4.2
Huey Cobra Helicopter	6.0	9.8	3.7	6.1
F-4 Aircraft	9.6	15.7	6.0	9.8
TU-16 Aircraft	20.8	34.1	13.0	21.3
C-5A Aircraft	41.8	68.3	26.1	42.7
Patrol Boat	8.5	13.9	3.4	5.0
Destroyer Class Ship	27.1	44.3	11.0	18.0
Field Trailer	6.2	10.2	3.9	6.4
POL Storage Tank	11.7	19.2	7.3	12.0
Pahlevi Dam	149.6	244.7	93.5	153.0
Golden Gate Bridge	481.3	787.6	300.8	492.3

Note: See text for assumptions!
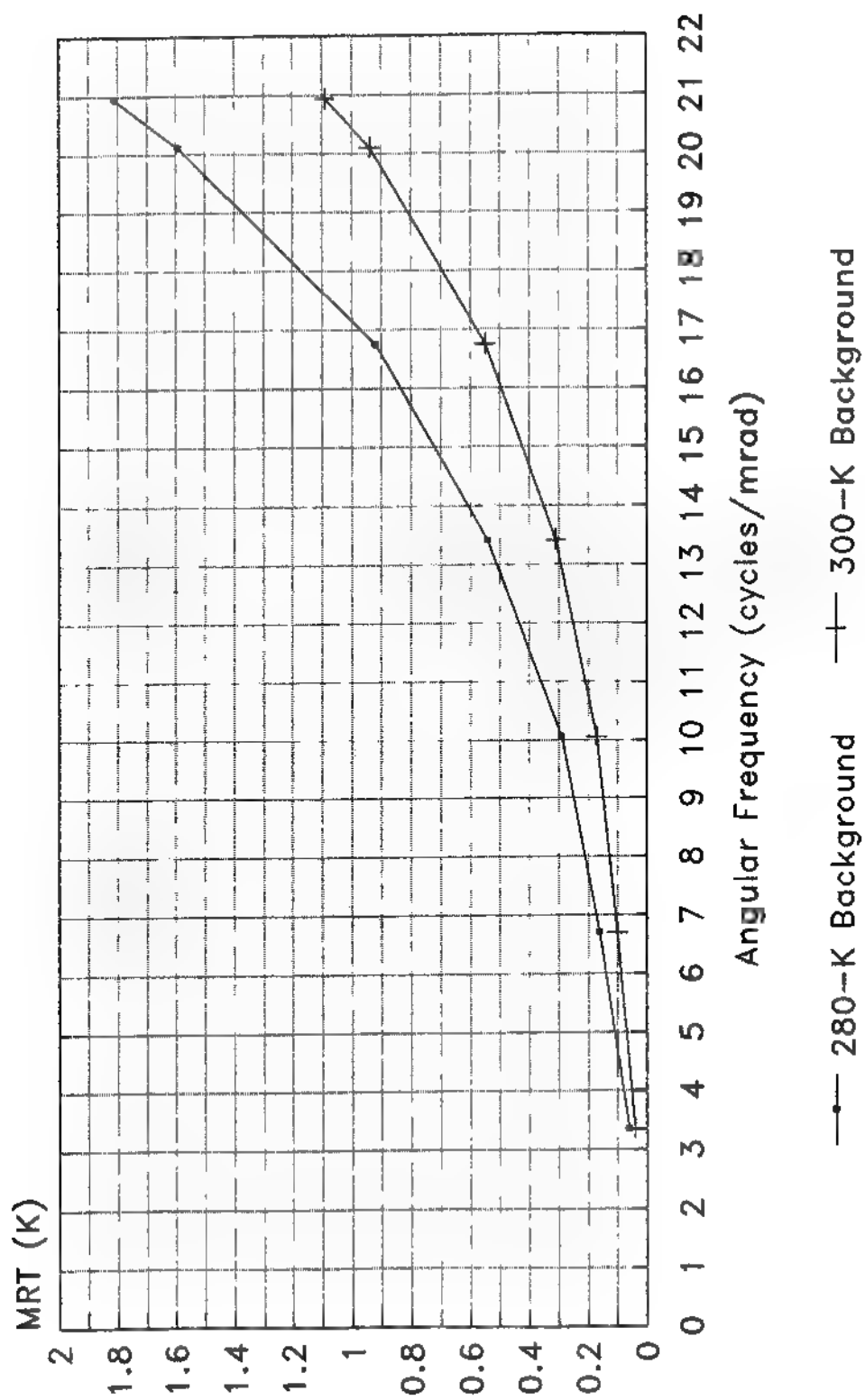
Data from LFS Report of 1/13/92

Figure 1. Predicted laboratory minimum resolvable temperature difference for IREO LOROPS

Ground resolution 37.5 ft
(1.6 cycles/mrad at 20 nmi)
11 blocks

Ground resolution 18.8 ft
(3.2 cycles/mrad at 20 nmi)
38 blocks

Ground resolution 15.0 ft
(4.1 cycles/mrad at 20 nmi)
57 blocks

Ground resolution 12.5 ft
(4.9 cycles/mrad at 20 nmi)
82 blocks

Ground resolution 9.4 ft
(6.5 cycles/mrad at 20 nmi)
149 blocks

Ground resolution 7.5 ft
(8.1 cycles/mrad at 20 nmi)
220 blocks

Ground resolution 5.9 ft
(10.3 cycles/mrad at 20 nmi)
357 blocks

Figure 2.   Block-type and graphic profile silhouettes of a
Forrest Sherman class destroyer

14

Ground resolution 37.5 ft
(1.6 cycles/mrad at 20 nmi)
11 blocks

Ground resolution 18.8 ft
(3.2 cycles/mrad at 20 nmi)
34 blocks

Ground resolution 15.0 ft
(4.1 cycles/mrad at 20 nmi)
56 blocks

Ground resolution 12.5 ft
(4.9 cycles/mrad at 20 nmi)
84 blocks

Ground resolution 9.4 ft
(6.5 cycles/mrad at 20 nmi)
146 blocks

Ground resolution 7.5 ft
(8.1 cycles/mrad at 20 nmi)
227 blocks

Ground resolution 5.9 ft
(10.3 cycles/mrad at 20 nmi)
367 blocks

Figure 3.   Block-type and graphic profile silhouettes of a
Kotlin class destroyer
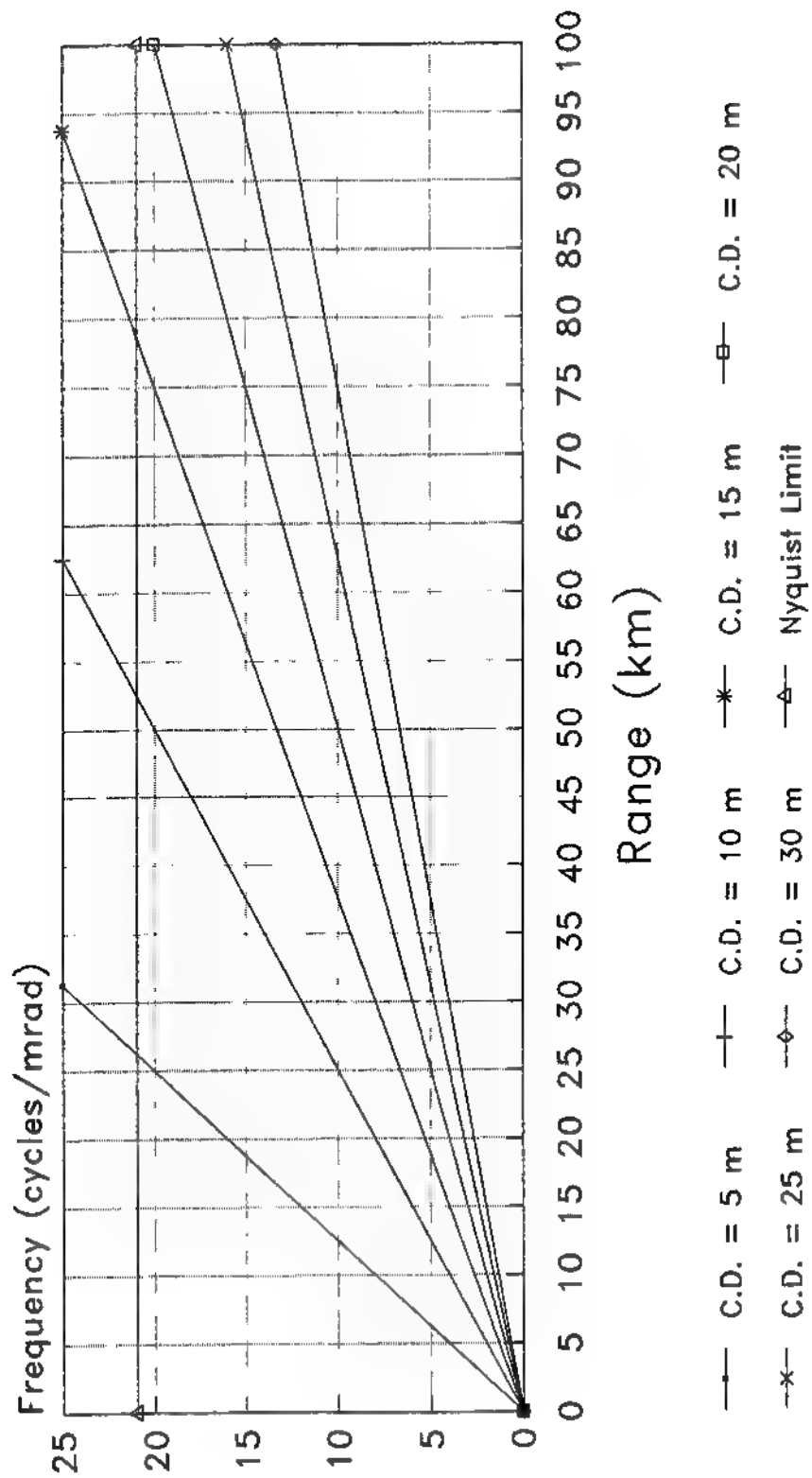
Figure 4.   Angular frequencies required for recognition of generic targets
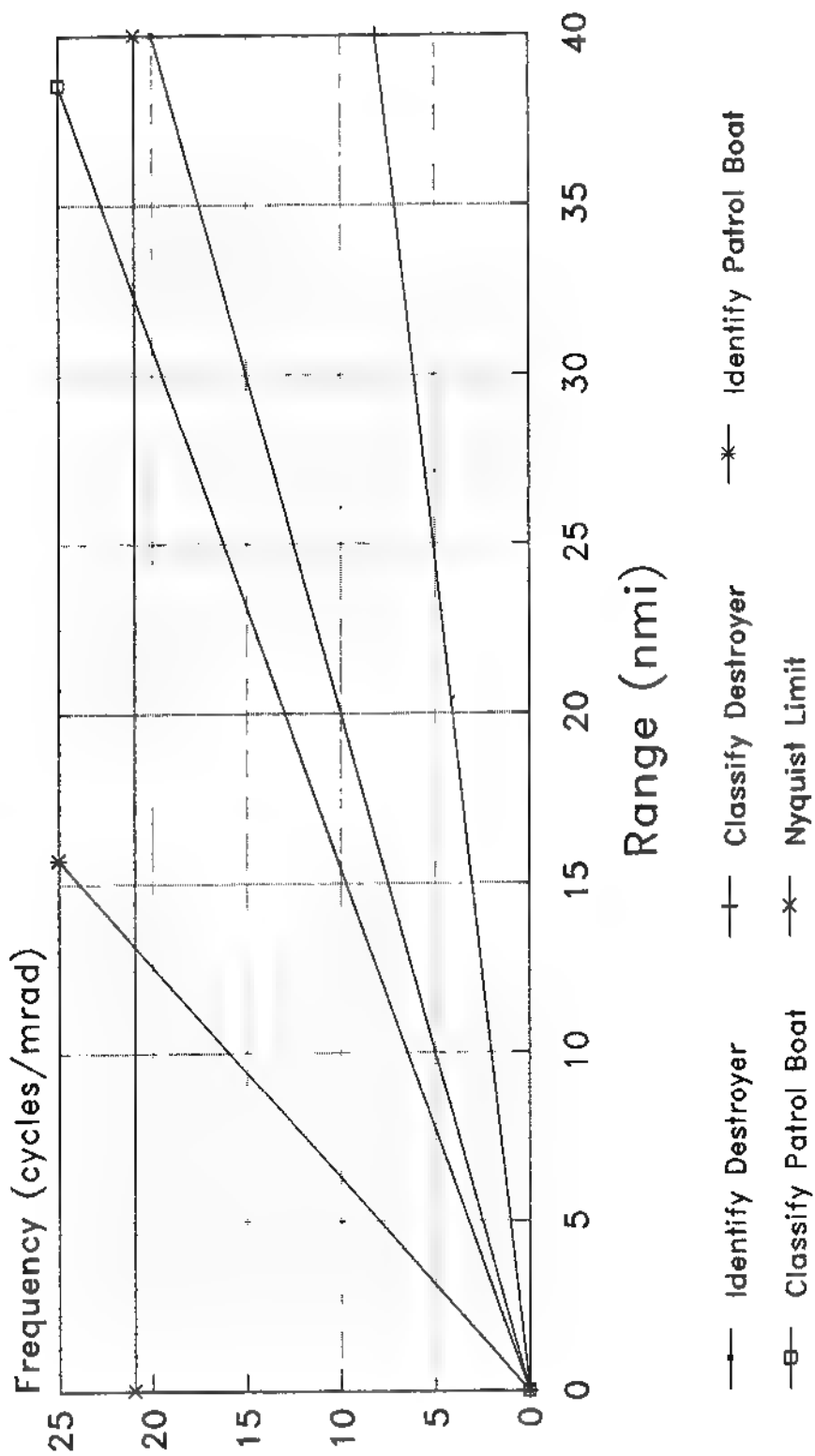
Beam aspect, 20.05 deg depression angle

Figure 5.   Angular frequencies required for classification and identification
of ships
Criteria: classification, 66 pixels/target area;
identification, 400 pixels/target area

17
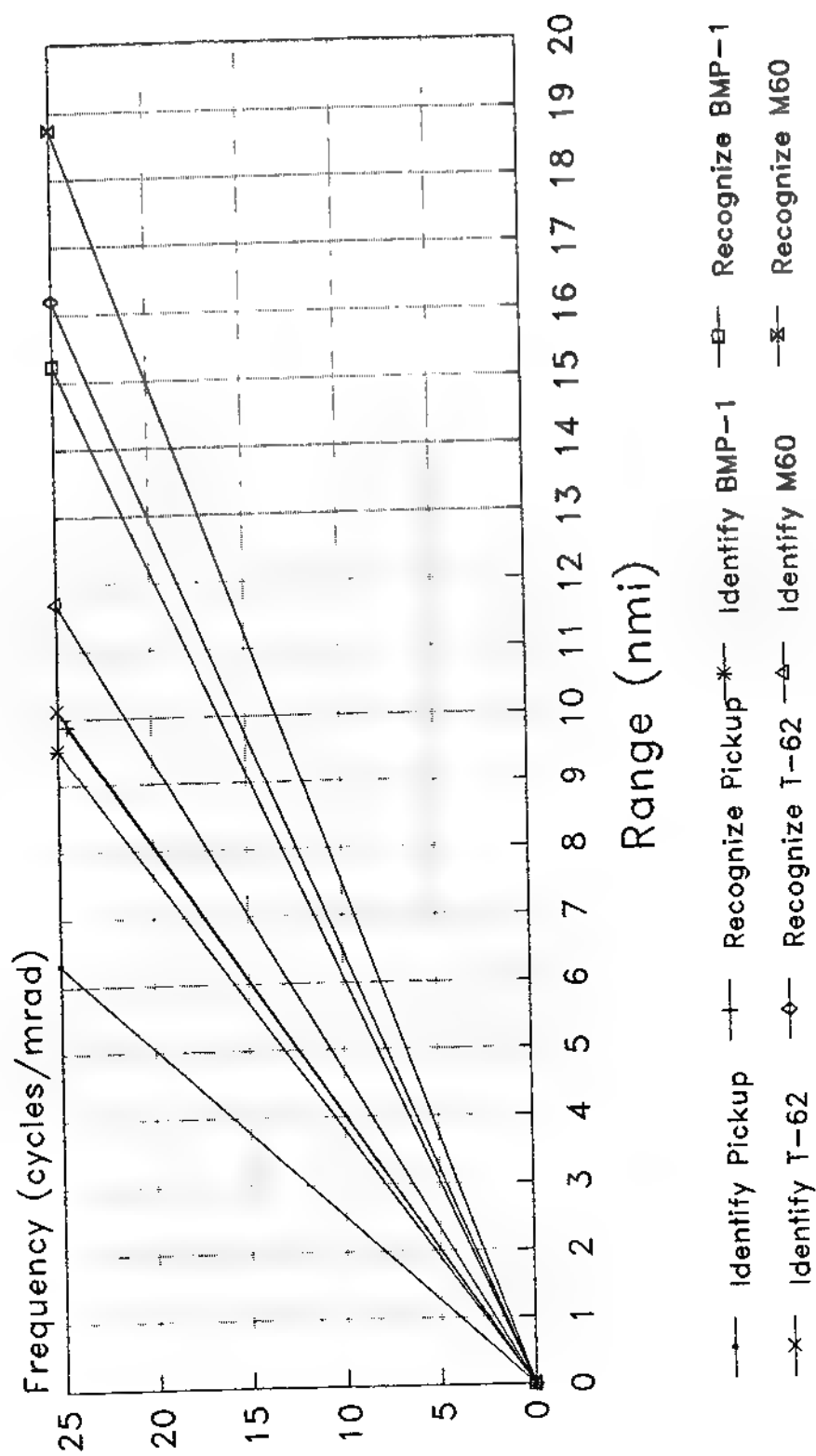
Figure 6. Angular frequencies required for recognition and identification of land vehicles
Criteria: recognition, 4.0 cycles/critical dimension
identification, 6.4 cycles/critical dimension
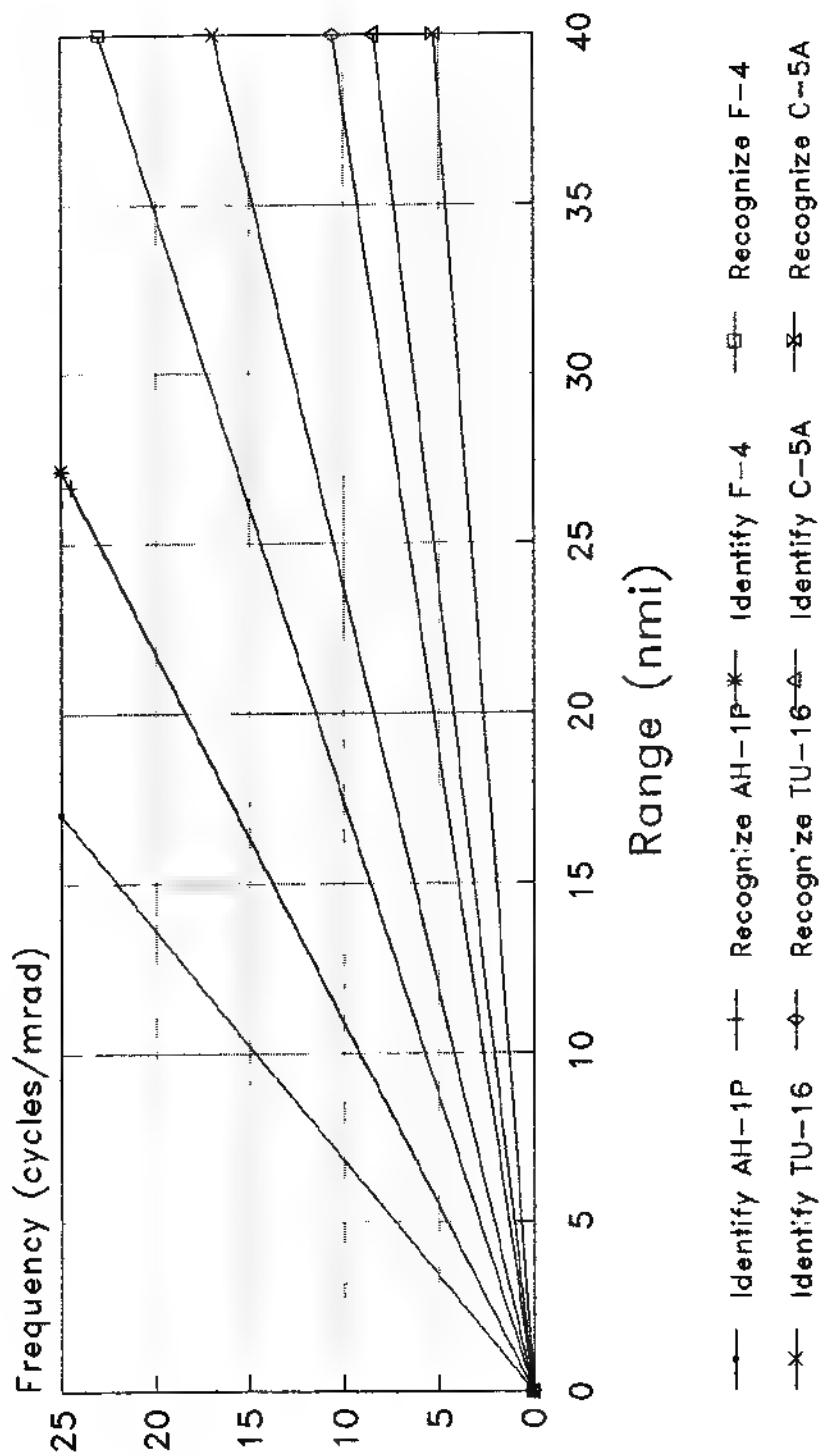
Beam aspect, 20.05 deg depression angle

Figure 7.   Angular frequencies required for recognition and identification
of aircraft on the ground
Criteria: recognition, 4.0 cycles/critical dimension
identification, 6.4 cycles/critical dimension
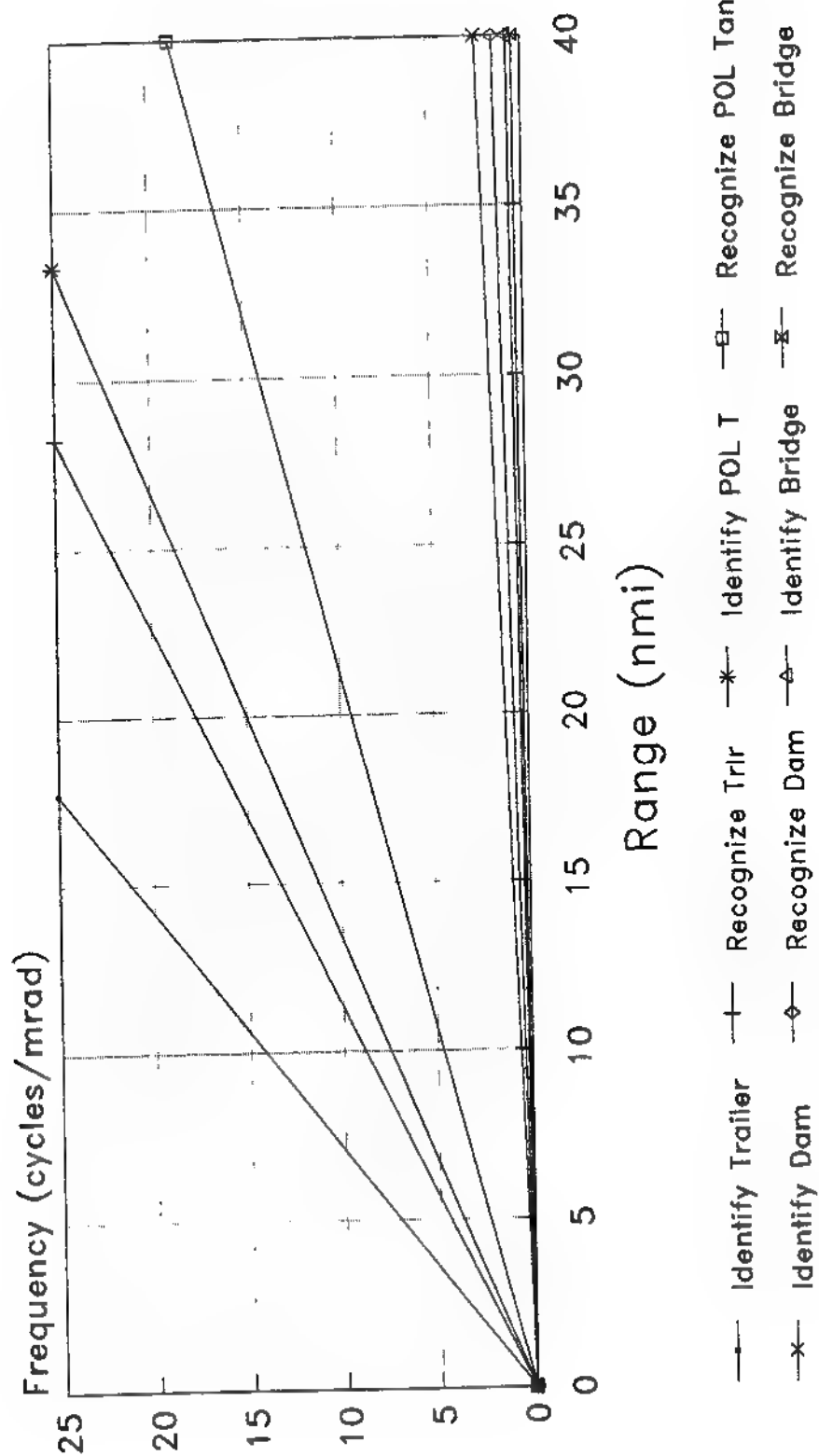
Beam aspect, 20.05 deg depression angle

Figure 8. Angular frequencies required for recognition and identification
of mostly fixed land targets
Criteria: recognition, 4.0 cycles/critical dimension
identification, 6.4 cycles/critical dimension
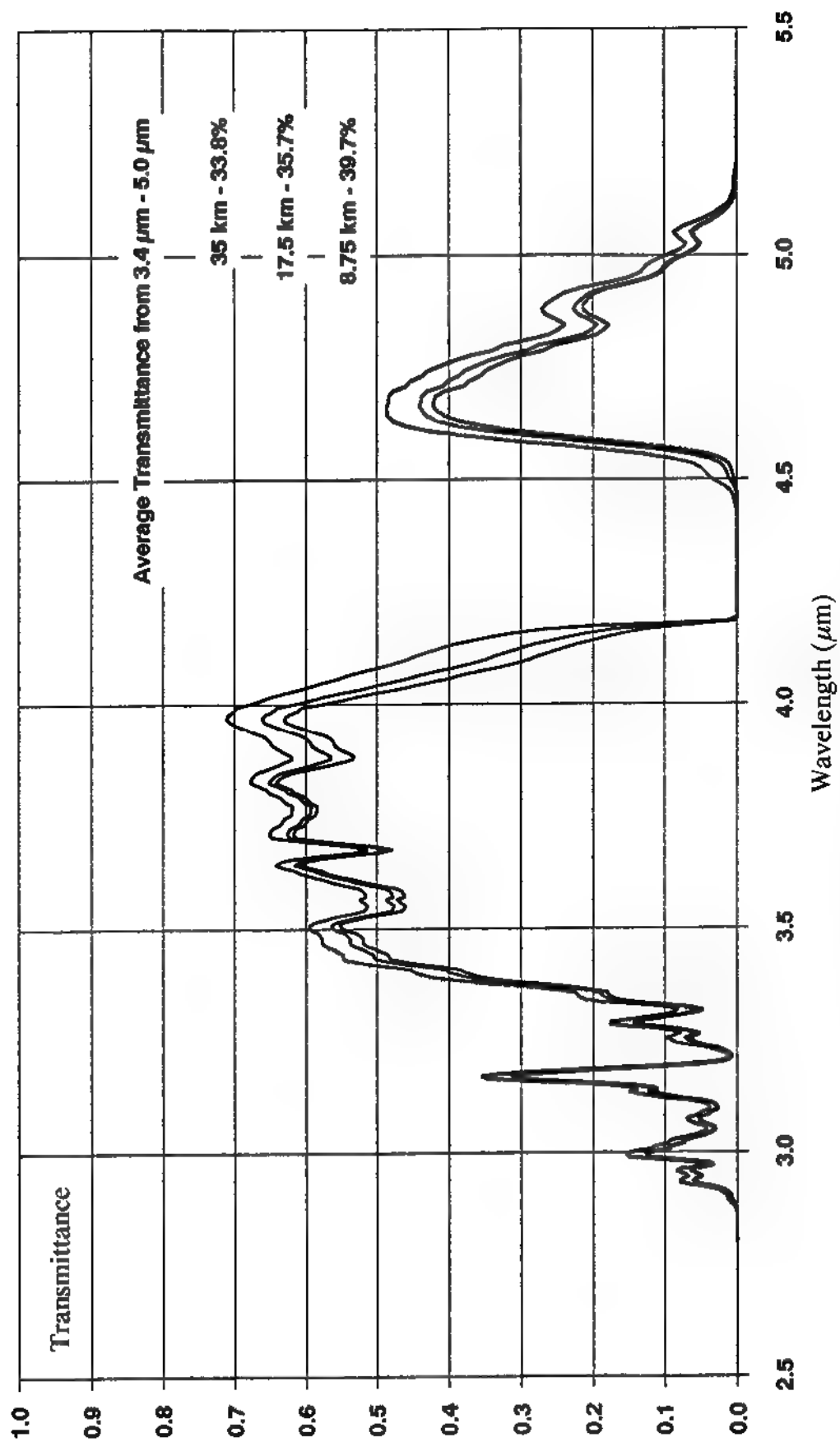
Figure 9. LOWTRAN 7 transmittance through 1976 U.S. standard atmosphere
Navy maritime aerosol model
Visibility 25 km
Slant ranges to surface: 8.75 km, 17.5 km, 35 km
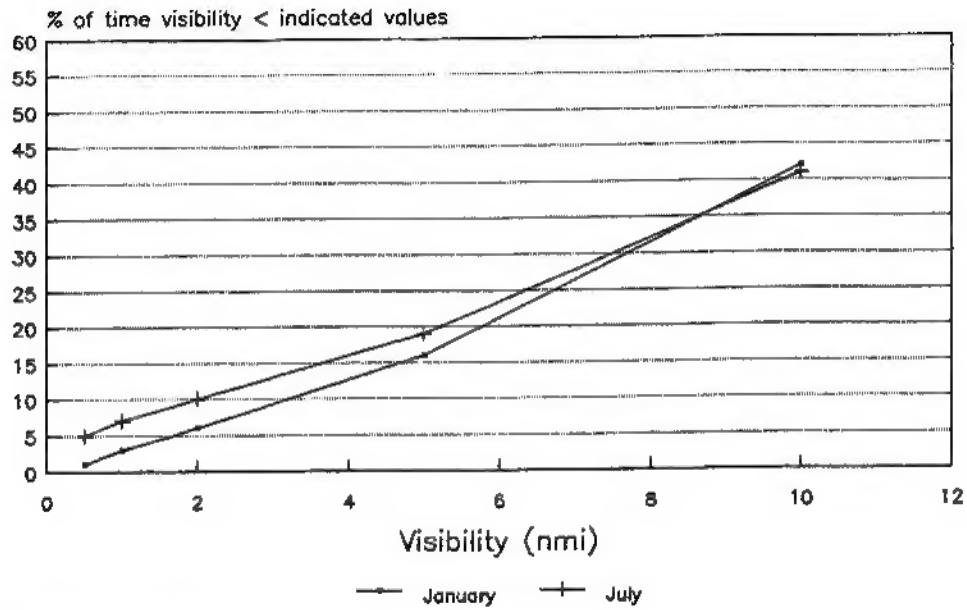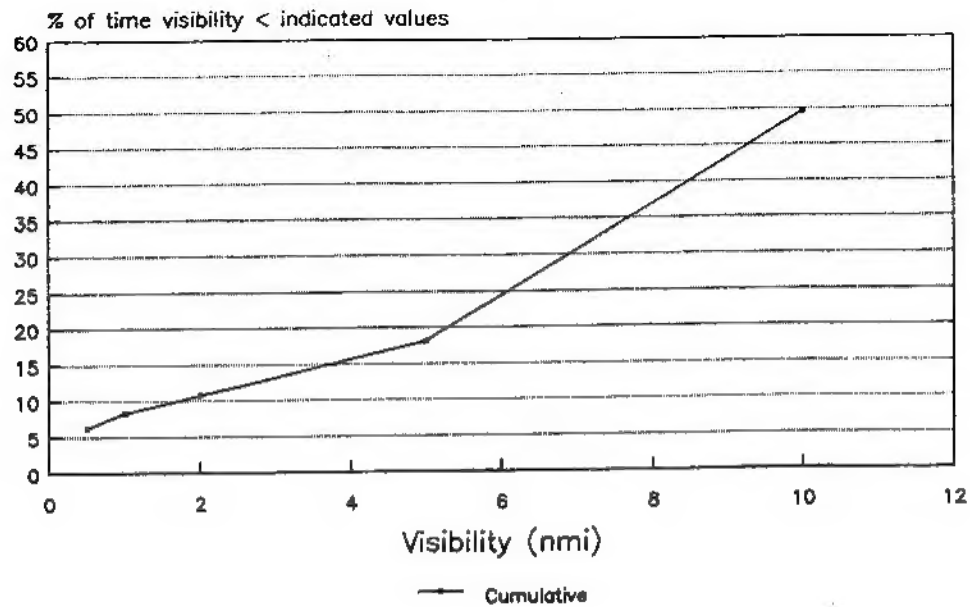Depression angle 20.05°
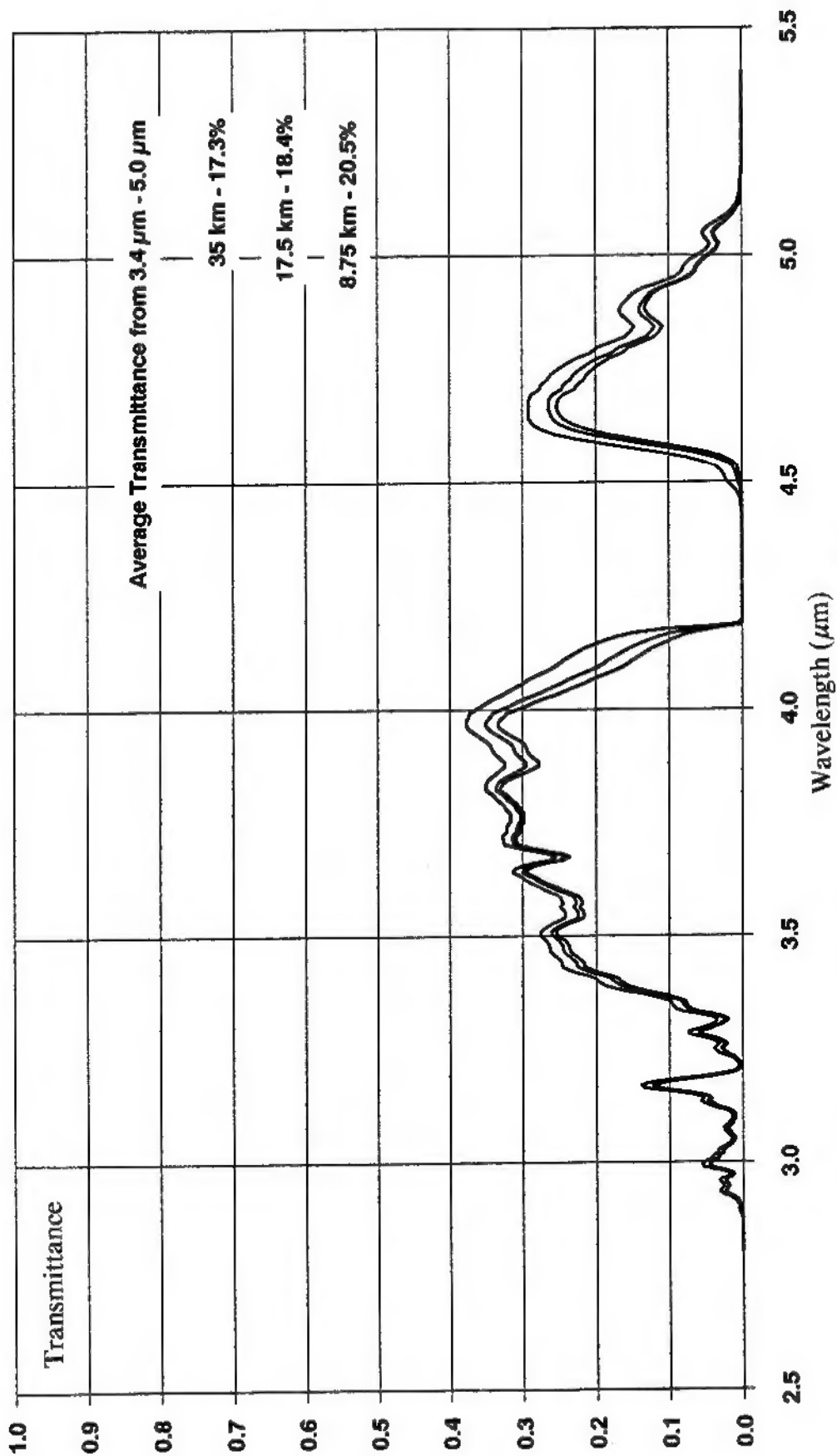
Figure 10. LOWTRAN 7 transmittance through 1976 U.S. standard atmosphere
Navy maritime aerosol model
Visibility 5 km
Slant ranges to surface: 8.75 km, 17.5 km, 35 km
Depression angle 20.05°

% of time visibility < indicated values

Figure 11. Visibility probabilities, Norwegian Sea, (66.0°N, 2.0°E)

% of time visibility < indicated values

Figure 12. Visibility probabilities, marine area near Boston, MA

% of time visibility < indicated values

40N–Coast, 72W–Coast, Annual
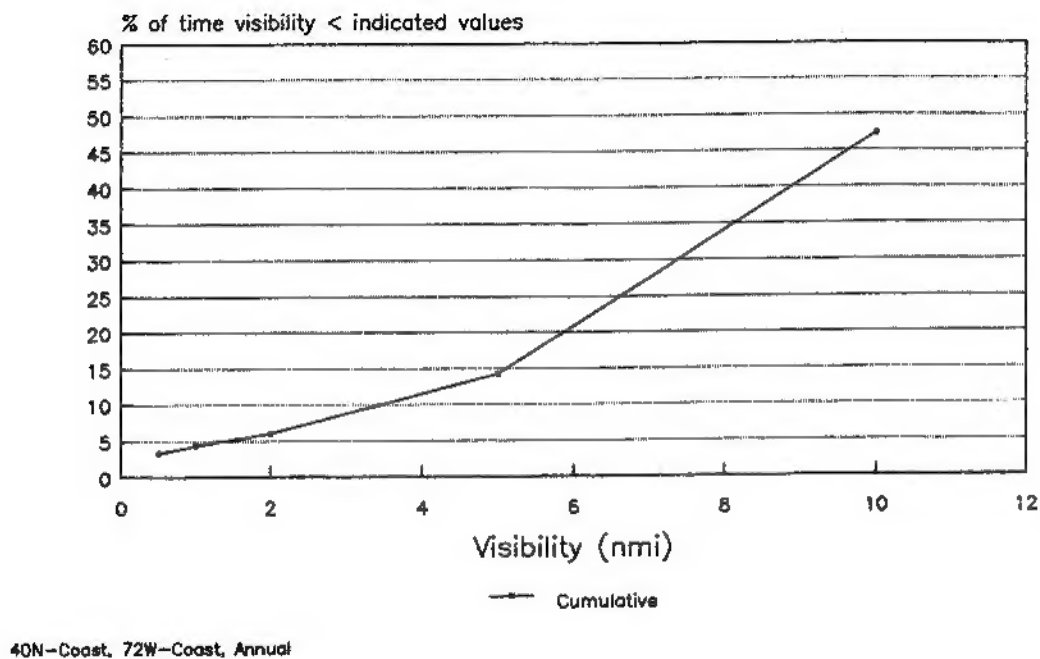
Figure 13. Visibility probabilities, marine area near New York, NY

% of time visibility < indicated values

36–40N, 72W–Coast, Annual
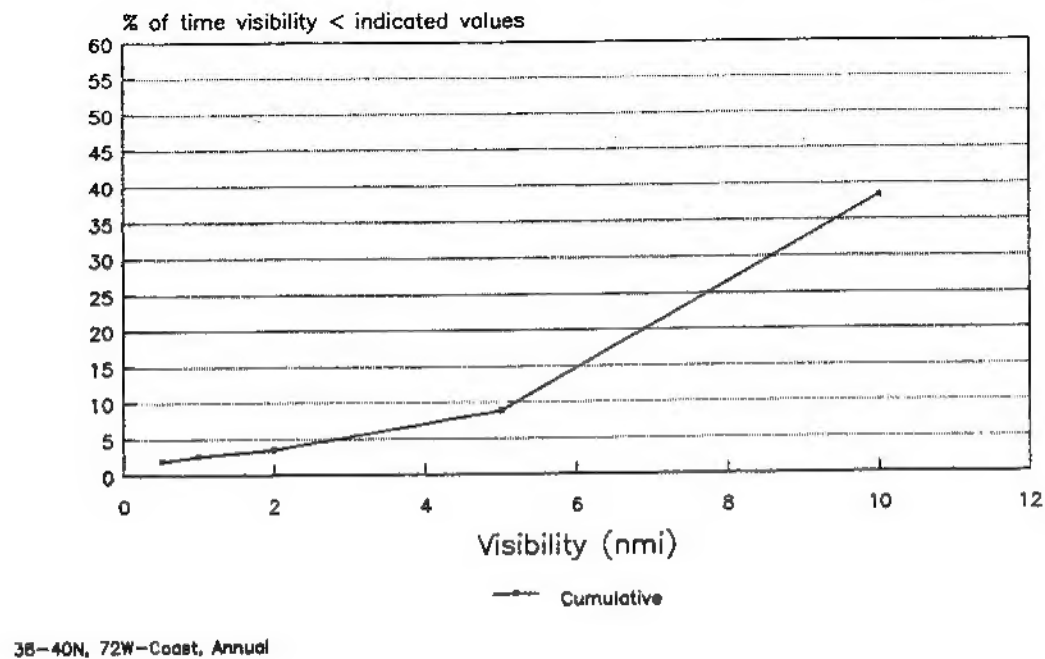
Figure 14. Visibility probabilities, marine area near Atlantic City, NJ

24

% of time visibility < indicated values

29-32N, 78W-Coast, Annual
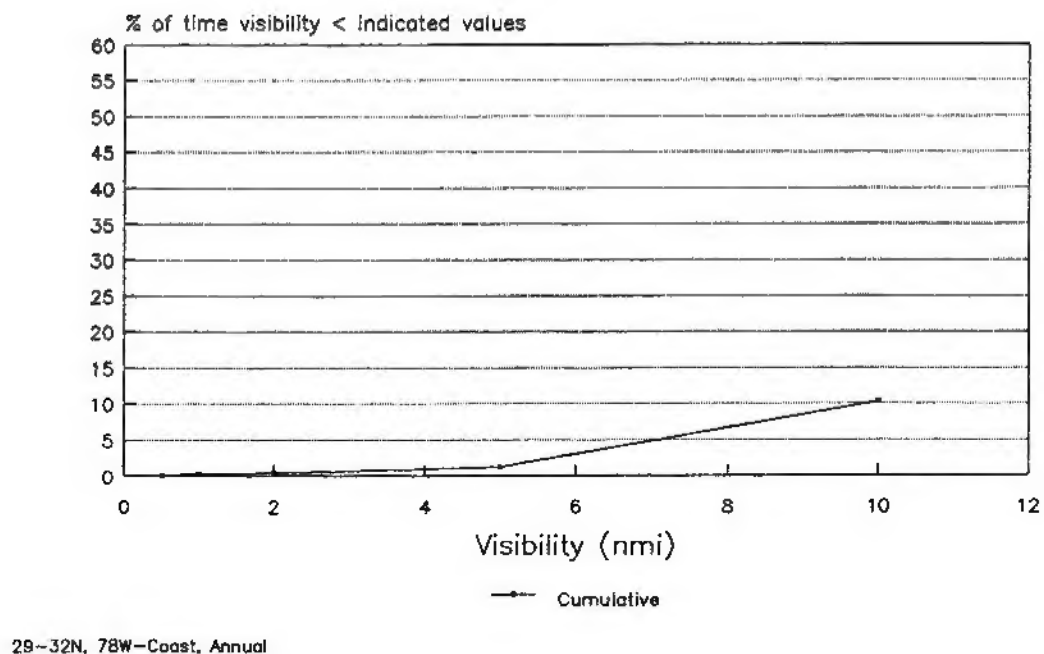
Figure 15. Visibility probabilities, marine area near Jacksonville, FL

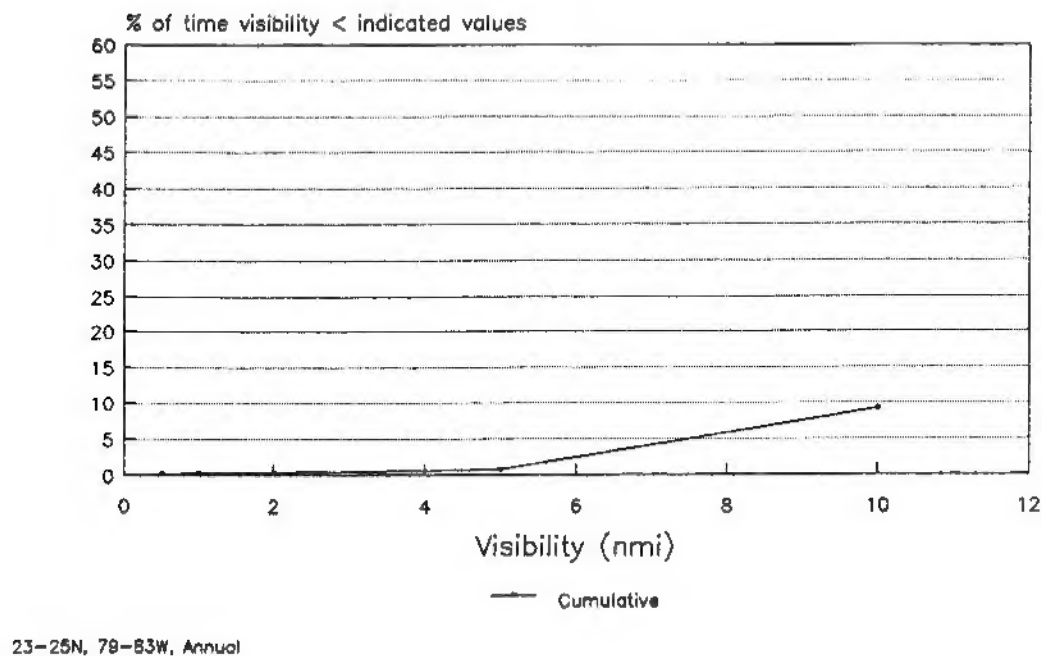
% of time visibility < indicated values

23-25N, 79-83W, Annual

Figure 16. Visibility probabilities, marine area near Key West, FL